

Argonne National Laboratory

**THE AXISYMMETRIC FREE-CONVECTION
HEAT TRANSFER ALONG A VERTICAL
THIN CYLINDER WITH CONSTANT
SURFACE TEMPERATURE**

by

R. Viskanta

PROPERTY OF
ANL-W Technical Library

LEGAL NOTICE

This report was prepared as an account of Government sponsored work. Neither the United States, nor the Commission, nor any person acting on behalf of the Commission:

- A. Makes any warranty or representation, expressed or implied, with respect to the accuracy, completeness, or usefulness of the information contained in this report, or that the use of any information, apparatus, method, or process disclosed in this report may not infringe privately owned rights; or*
- B. Assumes any liabilities with respect to the use of, or for damages resulting from the use of any information, apparatus, method, or process disclosed in this report.*

As used in the above, "person acting on behalf of the Commission" includes any employee or contractor of the Commission, or employee of such contractor, to the extent that such employee or contractor of the Commission, or employee of such contractor prepares, disseminates, or provides access to, any information pursuant to his employment or contract with the Commission, or his employment with such contractor.

ARGONNE NATIONAL LABORATORY
9700 South Cass Avenue
Argonne, Illinois

THE AXISYMMETRIC FREE-CONVECTION HEAT TRANSFER
ALONG A VERTICAL THIN CYLINDER
WITH CONSTANT SURFACE TEMPERATURE

by

R. Viskanta

Reactor Engineering Division

January 1963

Operated by The University of Chicago
under
Contract W-31-109-eng-38
with the
U. S. Atomic Energy Commission

TABLE OF CONTENTS

	<u>Page</u>
NOMENCLATURE	4
ABSTRACT	6
I. INTRODUCTION.	6
II. ANALYSIS.	7
General Considerations and Mathematical Formulation. . . .	7
Solution of the Problem for Small Values of the x-Parameter (ξ).	9
Solution of the Problem for Large Values of the x-Parameter (ξ).	10
Skin-Friction and Heat-Transfer Parameters	13
III. DISCUSSION OF RESULTS.	15
IV. CONCLUSIONS.	20
APPENDICES:	
A. Numerical Solution of the Perturbation Equations [Eqs. (13) and (14)].	22
B. Reduction of the Integral Equations [Eqs. (17) and (18)].	23
REFERENCES.	25
ACKNOWLEDGMENTS	26

LIST OF FIGURES

<u>No.</u>	<u>Title</u>	<u>Page</u>
1.	Physical Model and Coordinate System.	8
2.	Variation of the First Perturbation of the Dimensionless Velocity Distribution $f_1(\eta)$	16
3.	Variation of the First Perturbation of the Dimensionless Temperature Distribution $\theta_1(\eta)$	17
4.	Comparison of Local Nusselt Number between Cylinder and Flat Plate	18
5.	Comparison of Local Shear Stress between Cylinder and Flat Plate	19
6.	Variation of the Nusselt Number for the Cylinder Versus the x-Parameter	19
7.	Comparison of the Nusselt Numbers for Prandtl Number of 0.72	20

LIST OF TABLES

<u>No.</u>	<u>Title</u>	<u>Page</u>
1.	Temperature Gradients at the Surface of the Cylinder.	15

NOMENCLATURE

A	Function defined by Eq. (44)
a	Function defined by Eq. (41)
B	Function defined by Eq. (45)
b	Function defined by Eq. (42)
C	Function defined by Eq. (46)
c	Function defined by Eq. (43)
c_p	Specific heat at constant pressure
D	Function defined by Eq. (50)
d	Function defined by Eq. (49)
f	Dimensionless stream function defined by Eq. (8)
Gr	Grashof number based on the radius as a characteristic dimension, defined as $g\beta T_w - T_a r_0^3/\nu^2$
Gr_x	Grashof number based on the axial distance x as a characteristic dimension, defined as $g\beta T_w - T_a x^3/\nu^2$
g	Acceleration due to gravity
h	Local heat-transfer coefficient
\bar{h}	Average heat-transfer coefficient defined by Eq. (35)
K	Constant defined as $g\beta T_w - T_a r_0^2/2\nu$
k	Thermal conductivity
Nu	Nusselt number based on the radius of the cylinder as a characteristic dimension; see Eq. (32)
Nu_x	Nusselt number based on the axial distance along the cylinder as a characteristic dimension; see Eq. (33)
Pr	Prandtl number defined as $\mu c_p/k$
r	Radial coordinate
r_0	Radius of the cylinder
q	Local heat flux
T	Temperature
T_a	Ambient coolant temperature
T_w	Temperature at the wall of the cylinder
U	Parameter in Eq. (19)
u	Velocity of the coolant in the axial direction

v	Velocity of the coolant in the radial direction
x	Axial coordinate
y	Radial coordinate defined as $y = r - r_0$
α	Thermal diffusivity defined as $k/\rho c_p$
β	Coefficient of the volumetric expansion of the fluid
δ	Momentum boundary layer thickness defined by Eq. (21)
δ_t	Thermal boundary layer thickness
η	Dimensionless coordinate defined by Eq. (6)
θ	Dimensionless temperature defined by Eq. (9)
μ	Dynamic viscosity
ν	Kinematic viscosity
ξ	Dimensionless x-parameter defined by Eq. (7)
ρ	Density
σ	Function defined as $1/\text{Nu}$
τ	Shear stress at the surface
ψ	Stream function defined by Eq. (8)

Subscripts

fp	Refers to a flat plate
cyl	Refers to cylinder

Superscripts

'	Denotes differentiation with respect to variable η
---	---

THE AXISYMMETRIC FREE-CONVECTION HEAT TRANSFER ALONG A VERTICAL THIN CYLINDER WITH CONSTANT SURFACE TEMPERATURE

by

R. Viskanta

ABSTRACT

The subject of this study is the problem of laminar free-convection flow produced by a heated, vertical, circular cylinder for which the temperature at the outer surface of the cylinder is assumed to be uniform. The solution of the boundary-layer equations was obtained by two methods: (1) the perturbation method of Sparrow and Gregg, which is valid only for small values of the axial distance parameter ξ ; and (2) the integral method of Hama *et al.*, for large values of the parameter ξ . Heat-transfer results were calculated for Prandtl numbers (Pr) of 100, 10, 2, 1, 0.72, 0.1, 0.03, 0.02, and 0.01. It was found that the Nusselt numbers (Nu) for the cylinder were higher than those for the flat plate, and this difference increased as Pr decreased. It was also found that the perturbation method of solution of the free-convection boundary-layer equations becomes useless for small values of Pr because of the slow convergence of the series. The results obtained by the integral method were in good agreement with those calculated by the perturbation method for $Pr \approx 1$ and $0.1 < \xi < 1$ only; they deviated considerably for smaller values of ξ .

I. INTRODUCTION

The gravitational free convection from a number of typical geometries, such as the vertical flat plate, the horizontal tube, and the vertical circular cylinder, are important in industrial applications. Even though laminar free convection on a vertical plate has been a subject of study since 1881, there has been little study of laminar free-convection heat transfer from a vertical thin cylinder. Recently, the knowledge of heat transfer from a fuel pin (a circular cylinder) under free-convection conditions has become of particular importance in considerations of reactor safety. When the boundary-layer thickness is small compared with the radius of the cylinder, the effect of transverse curvature on the flow and heat transfer is negligible, and the velocity and temperature distributions

can be well approximated by the solution of the problem of the vertical flat plate. As the distance from the leading nose increases, the thickness of the boundary layer also increases, so that the effect of transverse curvature becomes no longer negligible, and the results for a vertical cylinder depart more and more from those of a flat plate.

The theoretical investigations of the axisymmetric free convection are primarily limited to the study of Sparrow and Gregg,⁽¹⁾ who solved the boundary-layer equations and obtained numerical results for Prandtl numbers of 0.72 and 1, as applicable for gases; and the more recent analytical and experimental study of Hama *et al.*,⁽²⁾ for Prandtl number 0.72, as applicable for air. References (1) and (2) also list other related work on free-convection problems. The solution of Sparrow and Gregg provides a very good approximation of the boundary-layer equations near the nose of the cylinder where the boundary-layer thickness is small compared with the radius of the cylinder. The solution is not expected to be applicable in the region far from the nose where the thickness of the boundary layer is comparable with or much larger than the radius of the cylinder. This is the case as shown analytically and verified experimentally by Hama *et al.*

This report presents a study of laminar free-convection heat transfer from a vertical thin cylinder at a constant surface temperature. The analyses of References (1) and (2) are extended to fluids with high and low Prandtl numbers. In the latter case, i.e., for liquid metals, the inertia terms in the momentum equation are not negligible in comparison with the viscous terms, and therefore the inertia terms have been retained in the momentum integral equation.

II. ANALYSIS

General Considerations and Mathematical Formulation

The physical model and coordinate system are indicated in Fig. 1. Two physical situations that come within the scope of the analysis are shown. In Fig. 1(a) the wall temperature T_w exceeds the ambient temperature T_a . For this case, due to buoyancy forces, an upward flow of fluid in the boundary layer is established. In Fig. 1(b) the wall temperature is cooler than the ambient temperature, and the flow of the fluid in the boundary layer is downward.

If the coordinate systems are taken as shown in Fig. 1, there is no distinction between the two problems and the method of analysis and the results for heat transfer are the same; thus, there is no need to treat the problems separately.

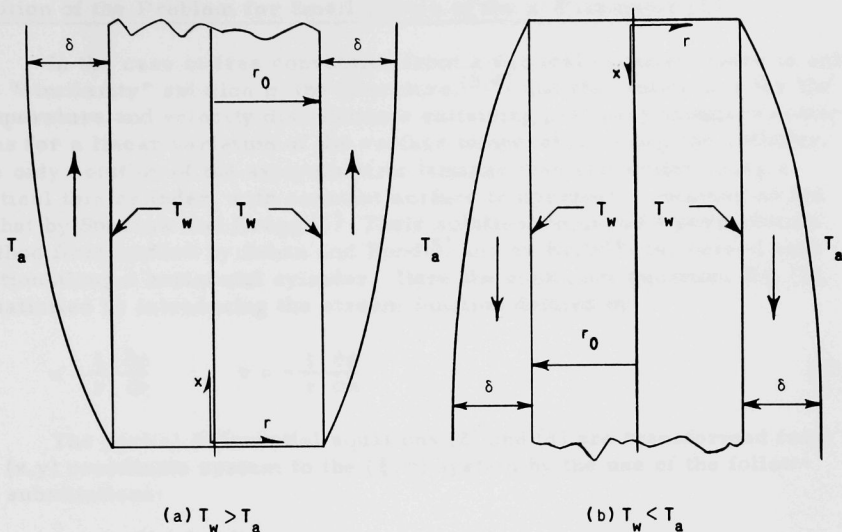


Fig. 1. Physical Model and Coordinate System

The basic conservation equations of mass, momentum, and energy for axisymmetric laminar free convection along a vertical cylinder, under the assumptions of boundary-layer approximations and constant physical properties, are given by

$$\frac{\partial}{\partial x} (ru) + \frac{\partial}{\partial r} (rv) = 0 \quad ; \quad (1)$$

$$u \frac{\partial u}{\partial x} + v \frac{\partial u}{\partial r} = \frac{\nu}{r} \frac{\partial}{\partial r} \left(r \frac{\partial u}{\partial r} \right) \pm g\beta (T - T_a) \quad ; \quad (2)$$

$$u \frac{\partial T}{\partial x} + v \frac{\partial T}{\partial r} = \frac{\alpha}{r} \frac{\partial}{\partial r} \left(r \frac{\partial T}{\partial r} \right) \quad . \quad (3)$$

Viscous dissipation and work against the gravity field have been neglected. In accord with the usual practice in free convection, the density has been considered a variable only in formulating the buoyancy term $[\pm g\beta(T - T_a)]$. The plus sign is associated with Fig. 1(a), whereas the minus sign is used with Fig. 1(b).

The boundary conditions to be satisfied are given by

$$\left. \begin{aligned} u = v = 0 \quad ; \quad T = T_w \text{ at } r = r_0 \\ u = 0 \quad ; \quad T = T_a \text{ at } r \rightarrow \infty \end{aligned} \right\} \quad (4)$$

Solution of the Problem for Small Values of the x-Parameter (ξ)

In the case of free convection from a vertical cylinder, there is only one "similarity" solution in the literature,^(3,4) and that solution is for the temperature and velocity distributions satisfying pertinent boundary conditions for a linear variation of the surface temperature along the cylinder. The only solution of the axisymmetric laminar free convection along a vertical thin cylinder, with constant surface temperature, obtained so far is that by Sparrow and Gregg.⁽¹⁾ Their solution employed a perturbation method first applied by Seban and Bond⁽⁵⁾ and by Kelly⁽⁶⁾ for forced convection along a horizontal cylinder. Here the continuity equation, Eq. (1), is satisfied by introducing the stream function defined by

$$u = \frac{1}{r} \frac{\partial \psi}{\partial r} \quad ; \quad v = -\frac{1}{r} \frac{\partial \psi}{\partial x} \quad . \quad (5)$$

The partial differential equations (2) and (3) are transformed from the (x,y) coordinate system to the (ξ, η) system by the use of the following substitutions:

$$\eta = \frac{Gr^{1/4} (x^2 - r_0^2)}{2^{3/2} r_0^{7/4} x^{1/4}} \quad , \quad (6)$$

$$\xi = \frac{2^{3/2}}{Gr^{1/4}} \left(\frac{x}{r_0} \right)^{1/4} = \frac{2^{3/2}}{Gr_x^{1/4}} \left(\frac{x}{r_0} \right) \quad , \quad (7)$$

$$\psi = \frac{Gr^{3/4} \nu r_0^{3/4} x^{1/4} f(\xi, \eta)}{2^{3/2}} \quad (8)$$

$$\theta = \frac{T - T_a}{T_w - T_a} \quad . \quad (9)$$

Then, by assuming that f and θ can be expanded in power series of ξ :

$$f(\xi, \eta) = \xi^2 [f_0(\eta) + \xi f_1(\eta) + \xi^2 f_2(\eta) + \dots +] \quad (10)$$

and

$$\theta(\xi, \eta) = \theta_0(\eta) + \xi \theta_1(\eta) + \xi^2 \theta_2(\eta) + \dots + \quad , \quad (11)$$

the partial differential equations in the coordinate system (ξ, η) reduced to the following systems of ordinary differential equations:

$$\left. \begin{aligned} \theta_0'' + 3 \text{Pr} f_0 \theta_0' &= 0 \\ f_0''' + 3 f_0 f_0'' - 2(f_0')^2 + \theta_0 &= 0 \end{aligned} \right\} \quad , \quad (12)$$

$$\left. \begin{aligned}
 \theta_1'' + \theta_0' + \eta \theta_0'' - \text{Pr}(f_0' \theta_1 - 4 f_1' \theta_0 - 3 f_0' \theta_1') &= 0 \\
 f_1''' + f_0'' + \eta f_0''' - 5 f_0' f_1' + 4 f_0'' f_1 + 3 f_1'' f_0 + \theta_1 &= 0
 \end{aligned} \right\} , \quad (13)$$

$$\left. \begin{aligned}
 \theta_2'' + \theta_1' + \eta \theta_1'' - \text{Pr}(f_1' \theta_1 + 2 f_0' \theta_2 - 5 f_2' \theta_0 - 4 f_1' \theta_1' - 3 f_0' \theta_2') &= 0 \\
 f_2''' + f_1'' + \eta f_1''' - 6 f_0' f_2' - 3(f_1')^2 + 5 f_0'' f_2 + 4 f_1'' f_1 + 3 f_2'' f_0 + \theta_2 &= 0
 \end{aligned} \right\} , \quad (14)$$

in which the primes denote differentiation with respect to η .

The boundary conditions, Eq. (4), become in the coordinate system of (ξ, η)

$$\left. \begin{aligned}
 f_0 = f_0' &= 0 \quad , \quad \theta_0 = 1 \text{ at } \eta = 0 \\
 f_0' = \theta_0' &= 0 \text{ at } \eta \rightarrow \infty
 \end{aligned} \right\} , \quad (12a)$$

$$\left. \begin{aligned}
 f_1 = f_1' &= \theta_1 = 0 \text{ at } \eta = 0 \\
 f_1' = \theta_1' &= 0 \text{ at } \eta \rightarrow \infty
 \end{aligned} \right\} , \quad (13a)$$

$$\left. \begin{aligned}
 f_2 = f_2' &= \theta_2 = 0 \text{ at } \eta = 0 \\
 f_2' = \theta_2' &= 0 \text{ at } \eta \rightarrow \infty
 \end{aligned} \right\} . \quad (14a)$$

Additional mathematical details can be found in Reference (1).

The zeroth-order approximation, Eq. (12), and the corresponding boundary conditions given in Eq. (12a) are identical with the differential equations for free convection along a vertical flat plate. Numerical solutions of these equations covering a large range of Prandtl numbers have been tabulated in detail.^(7,8) The solution of Eqs. (13) and (14), subject to the boundary conditions, Eqs. (13a) and (14a), respectively, is discussed in Appendix A.

Solution of the Problem for Large Values of the x-Parameter (ξ)

Since the x-parameter (ξ) is essentially a ratio of the thickness of the thermal boundary layer to the radius of the cylinder, it is expected from the nature of the expansion of $f(\xi, \eta)$ and $\theta(\xi, \eta)$ in power series of ξ that the Sparrow and Gregg solution should provide a good approximation near the leading edge, where the thickness of the thermal boundary layer is small in comparison with the radius of the cylinder. The radius of convergence of the series given by Eqs. (10) and (11) is not known; however,

it is not expected to be greater than one ($\xi < 1$). Therefore, the results⁽¹⁾ will not be applicable in the region far from the stagnation point, where $\xi > 1$ and the boundary-layer thickness is much larger than the radius of the cylinder. For this reason, the Karman-Pohlhausen integral method, as extended by Glauert and Lighthill,⁽⁹⁾ Mark,⁽¹⁰⁾ and Hama *et al.*,⁽²⁾ will be used to obtain an approximate solution for large values of the x-parameter (ξ).

It is assumed⁽¹¹⁾ that the common boundary-layer thickness (δ) can be used for both the momentum and thermal boundary layers. This assumption has its justification in that the results of calculations based on the assumption agree with those from exact solutions of the boundary-layer differential equations. Other authors,^(12,13) in their studies of free-convection problems, have assumed that the thickness of the thermal boundary layer, δ_t , is different from the thickness of the momentum boundary layer, δ , and these change with the Prandtl number. However, Merk⁽¹⁴⁾ points out that $\delta_t/\delta = 1$ for $Pr \leq 1$ and that $\delta_t/\delta < 1$ for $Pr > 1$. He further states that "it is not reasonable to assume that $\delta_t > \delta$, since this would mean that there are regions in which the temperature field differs from that of the surrounding fluid, and that in these regions buoyant force is present (in free convection, the velocity is caused by buoyant forces). Hence, from the physical point of view, it is clear that the upper bound δ_t/δ is given by (the number) 1." The exact (numerical) solutions of boundary-layer equations for free convection along a vertical flat plate, with low Prandtl number coolants, substantiate this conclusion.⁽⁸⁾

The integration of the basic equations (2) and (3) from the wall to the edge of the boundary layer with respect to r , after multiplying by r , and utilizing the boundary conditions given by Eq. (4), and the continuity equation (1), yields the integral equations

$$\frac{d}{dx} \int_{r_0}^{r_0+\delta} u^2 r \, dr = \pm g \beta (T_w - T_a) \int_{r_0}^{r_0+\delta} \theta r \, dr - \nu r_0 \left(\frac{\partial u}{\partial r} \right)_{r_0} \quad (15)$$

and

$$\frac{d}{dx} \int_{r_0}^{r_0+\delta} u \theta r \, dr = - \alpha r_0 \left(\frac{\partial \theta}{\partial r} \right)_{r_0}, \quad (16)$$

where θ is the dimensionless temperature. If a new independent variable, $y = r - r_0$, is introduced, Eqs. (15) and (16) become

$$\frac{d}{dx} \int_0^\delta u^2(r_0+y) \, dy = \pm g \beta (T_w - T_a) \int_0^\delta \theta(r_0+y) \, dy - r_0 \nu \left(\frac{\partial u}{\partial y} \right)_0 \quad (17)$$

and

$$\frac{d}{dx} \int_0^\delta u \theta(r_0 + y) dy = - \alpha r_0 \left(\frac{\partial \theta}{\partial y} \right)_0 . \quad (18)$$

In applying the Karman-Pohlhausen method of solution to axisymmetric problems, Glauert and Lighthill⁽⁹⁾ and Hama et al.,⁽²⁾ emphasize the importance of a proper profile whose behavior near the solid surface is realistic. According to Hama et al., the velocity profile is written as

$$u = K \left[U - \left(\frac{y}{r_0} \right) \right] \ln \left(\frac{y + r_0}{r_0} \right) . \quad (19)$$

The order of error in Eq. (19) is $O(y/r_0)^3$. The temperature profile is given by

$$\theta = 1 - Nu \ln \left(\frac{y + r_0}{r_0} \right) . \quad (20)$$

The temperature distribution near the wall is correct to the order of $O(y/r_0)^4$. The thickness of the thermal boundary layer is related to the Nusselt number (Nu) by the relation

$$\delta/r_0 = \exp(1/Nu) - 1 . \quad (21)$$

The coefficients U and Nu, which are functions of x, are found from the boundary conditions of the problem and the integrated momentum and energy equations.

The terms on the left-hand side of the momentum equation, Eq. (2) or (17), are the inertia terms. They are rather insignificant in the free-convection problems unless the Prandtl number is extremely small, such as in the case of liquid metals; therefore, it is not permissible to omit the inertia terms in the present analysis.

The functions representing the velocity, Eq. (19), and temperature distributions, Eq. (20), are introduced into Eqs. (17) and (18), and after integrations and differentiations are carried out (see Appendix B) there results

$$a \frac{dU}{d\xi} + b \frac{d\sigma}{d\xi} = d \quad (22)$$

and

$$A \frac{dU}{d\xi} + B \frac{d\sigma}{d\xi} = D \quad (23)$$

with the initial conditions:

$$U = \sigma = 0, \text{ for } \xi = 0 \quad . \quad (24)$$

Since the differential equations are singular at $\xi = 0$ in the numerical solution of Eqs. (22) and (23), it was only possible to approach the origin to within ϵ , estimate U and σ at $\xi = \epsilon$, and proceed with the numerical integration from that point on. The error introduced by this procedure could not be estimated. The Runge-Kutta method was used for the numerical solution of the differential equations.

Skin-Friction and Heat-Transfer Parameters

The local skin friction is obtained by applying the Newtonian shear formula:

$$\tau = \mu \left(\frac{\partial u}{\partial r} \right)_{r=r_0} \quad . \quad (25)$$

The velocity component u in the x -direction can be expressed in terms of the dimensionless stream function as

$$u = \frac{Gr\nu}{4r_0} \left(\frac{\partial f}{\partial \eta} \right) \quad . \quad (26)$$

In terms of dimensionless variables, the skin-friction parameter can be expressed as

$$\frac{\tau}{\frac{1}{2} \rho Gr (\nu/r_0)^2} = \frac{f''(0)}{\xi} = \xi [f_0''(0) + \xi f_1''(0) + \xi^2 f_2''(0) + \dots] \quad . \quad (27)$$

Equation (27) can be rewritten as the ratio of the shear stress for a cylinder (cyl) to that for a flat plate (fp) in the form

$$\frac{\tau_{\text{cyl}}}{\tau_{\text{fp}}} = \left[1 + \xi \frac{f_1''(0)}{f_0''(0)} + \xi^2 \frac{f_2''(0)}{f_0''(0)} + \dots + \right] \quad , \quad (28)$$

where

$$\frac{\tau_{\text{fp}}}{\rho [4Gr_x]^{1/4} (\nu/x)^2} = f_0''(0) \quad . \quad (29)$$

The local heat-transfer coefficient is defined as

$$h \equiv \frac{q}{(T_w - T_a)} = - \frac{k}{(T_w - T_a)} \left(\frac{\partial T}{\partial r} \right)_{r=r_0} \quad . \quad (30)$$

In terms of the dimensionless variables defined by Eqs. (6) and (9), the relation for h becomes

$$h = - \frac{k Gr^{1/4}}{2^{1/2} r_0^{3/4} x^{1/4}} \left(\frac{\partial \theta}{\partial \eta} \right)_{\eta=0} \quad (31)$$

The Nusselt number Nu , based on the radius of the cylinder as the characteristic dimension, is defined as

$$Nu \equiv \frac{hr_0}{k} = \frac{q}{(T_w - T_a)} \frac{r_0}{k} \quad (32)$$

The local Nusselt number Nu_x , based on the axial distance x as the characteristic dimension, is obtained from the definition of Eq. (32) and expression of Eq. (31) with the help of Eq. (11) as

$$Nu_x = Nu \left(\frac{x}{r_0} \right) = - \frac{1}{2^{1/2}} Gr_x^{1/4} [\theta'_0(0) + \xi \theta'_1(0) + \xi^2 \theta'_2(0) + \dots] \quad (33)$$

Since the first term on the right-hand side of Eq. (33) represents the local Nusselt number for the flat plate, Eq. (33) can be rewritten as the ratio of a local Nusselt number for the cylinder to that for the flat plate:

$$\frac{Nu_{x,cyl}}{Nu_{x,fp}} = 1 + \xi \frac{\theta'_1(0)}{\theta'_0(0)} + \xi^2 \frac{\theta'_2(0)}{\theta'_0(0)} + \dots \quad (34)$$

The average heat-transfer coefficient over a length x is defined as

$$\bar{h} = \frac{1}{x} \int_0^x h \, dx \quad (35)$$

If the indicated integration is performed and an average Nusselt number \bar{Nu}_x , based on the distance x as the characteristic dimension, is defined, there results

$$\bar{Nu}_x \equiv \frac{\bar{h}x}{k} = - \frac{2^{3/2}}{3} Gr_x^{1/4} \left[\theta'_0(0) + \frac{3}{4} \xi \theta'_1(0) + \frac{3}{5} \xi^2 \theta'_2(0) + \dots \right] \quad (36)$$

Again, the first term on the right-hand side of Eq. (36) is the average Nusselt number for a flat plate.

III. DISCUSSION OF RESULTS

From the solution of Eqs. (12) through (14), the essential information needed in the heat-transfer calculations includes $\theta_1'(0)$ and $\theta_2'(0)$. These results are listed in Table 1 with the values^(7,8) of $\theta_0'(0)$. There are two aspects of these results which should be mentioned: first, that $\theta_1'(0)$ varies only slightly with the Prandtl number over the very wide range considered here; and secondly, the large magnitudes of $\theta_1'(0)/\theta_0'(0)$ and $\theta_2'(0)/\theta_0'(0)$ for small Prandtl numbers. Thus, even for small ξ values ($\xi = 0.1$) the second and third terms of the series begin to be important. In the perturbation method of Sparrow and Gregg as applied to liquid metals, the truncation of the series after the third term appears to be in question, even for values of $\xi < 0.3$; therefore, no effort was made to obtain solutions for $Pr < 0.01$.

Table 1

TEMPERATURE GRADIENTS AT THE SURFACE OF THE CYLINDER

Pr	$\theta_0'(0)$	$\theta_1'(0)$	$\theta_2'(0)$	$\theta_1'(0)/\theta_0'(0)$	$\theta_2'(0)/\theta_0'(0)$
100	-2.1913	-0.2236		0.1020	
10	-1.1694	-0.2281		0.1347	
2	-0.7165	-0.2251	0.0206	0.3141	-0.0288
1	-0.5671	-0.2239	0.0262	0.4034	-0.0462
0.72	-0.5046	-0.2230	0.0298	0.4421	-0.0591
0.1	-0.2301	-0.2217	0.0810	0.6935	-0.3521
0.03	-0.1346	-0.2225	0.1525	1.6523	-1.1324
0.02	-0.1117	-0.2218	0.1811	1.9866	-1.6128
0.01	-0.0812	-0.2259	0.2051	2.7820	-2.5259

For completeness, the first perturbation of the velocity and temperature distributions (f_1' and θ_1) obtained are presented (Figs. 2 and 3, respectively) as functions of η for various values of Prandtl number. Both the minimum and the maximum values of the first perturbations of the dimensionless velocity and temperature distributions occur at larger values of the argument η as the Prandtl number decreases. The θ_1 function is related to the temperature distribution by Eq. (9), whereas the f_1' function is related to the velocity component u by Eqs. (26) and (10).

The ratio of the local Nusselt number for a cylinder to that for a flat plate is shown in Fig. 4. Three trends evident from Fig. 4 are: (1) that, for a fixed Prandtl number, the Nusselt number for a cylinder deviates more and more from the Nusselt number for a flat plate as ξ increases; (2) that, at a fixed value of the x -parameter (ξ), there are greater deviations of $Nu_{x,cyl}$ from $Nu_{x,fp}$ as the Prandtl number decreases; and

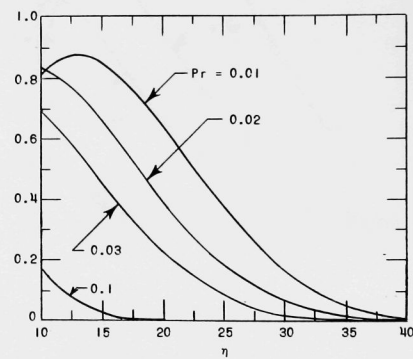
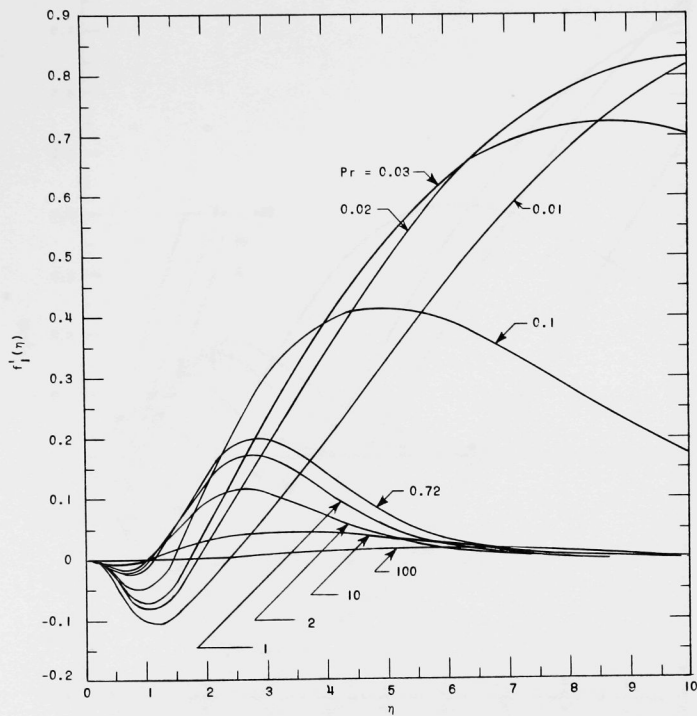


Fig. 2. Variation of the First Perturbation of the Dimensionless Velocity Distribution $f_1'(\eta)$

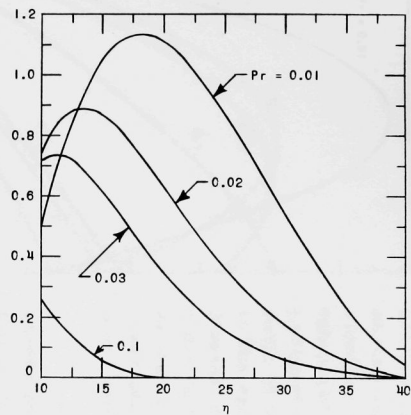
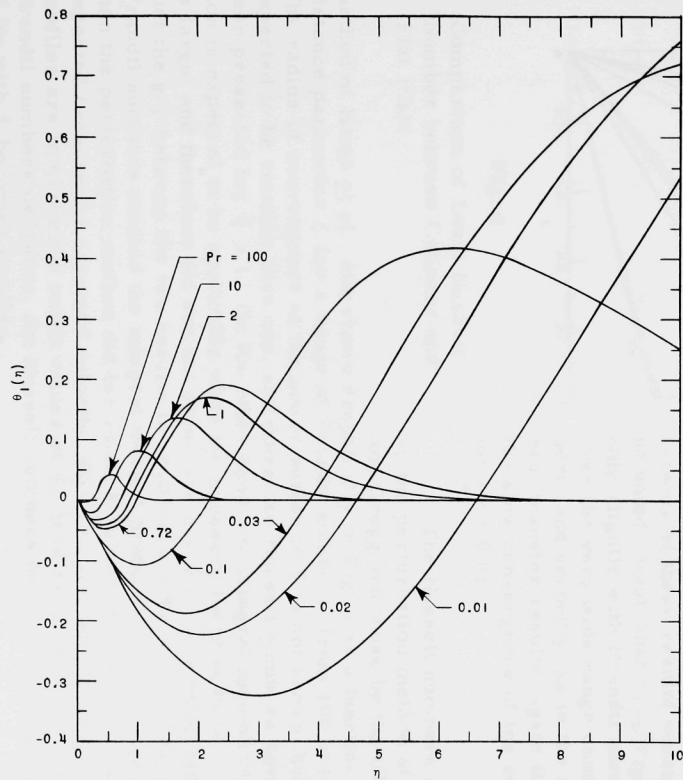


Fig. 3. Variation of the First Perturbation of the Dimensionless Temperature Distribution $\theta_1(\eta)$

- (3) that the perturbation method of solution of the boundary-layer equations becomes useless for $Pr < 0.1$ because of slow convergence of the power-series expansion of both the dimensionless stream function $f(\xi, \eta)$ and temperature $\theta(\xi, \eta)$. Since the x -parameter (ξ) is proportional to the ratio of the boundary-layer thickness to the radius of the cylinder, the Nusselt numbers for a cylinder are close to those for a flat plate, and as the thickness of the boundary layer increases the $Nu_{x, cyl}$ deviates more and more from $Nu_{x, fp}$.

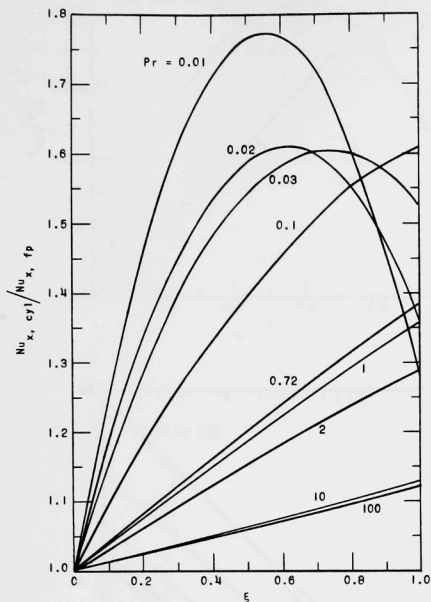


Fig. 4

Comparison of Local Nusselt Number between Cylinder and Flat Plate

The ratio of the local shear stress for the cylinder to that for a flat plate is shown in Fig. 5 for $Pr = 100$ and 0.01 . There are two aspects of these results which should be noted: first, that τ_{cyl}/τ_{fp} varies only slightly with Prandtl number over the very wide range considered here; and secondly, as in the case of heat transfer results, again there is the slow convergence of the series for $Pr = 0.01$.

The Nusselt numbers predicted by the perturbation method of Sparrow and Gregg and those by the integral

method of Hama *et al.*, are shown graphically in Fig. 6 as a function of the distance parameter ξ for a range of Prandtl numbers (from 100 to 0.01). The radius of convergence at the power series in ξ is not known, but it is expected to be smaller than one, and therefore Nusselt numbers have not been presented for $\xi > 1$. On the other hand, the integral method of solution is expected to be applicable when the boundary layer is thick, i.e., ξ is large, and therefore Nu are not shown for $\xi < 0.5$. It is seen, however, that the gap between the two results is smallest for $Pr \approx 1.0$. For all Prandtl numbers studied the integral method predicted larger values of Nu than the perturbation method did for small ξ values ($\xi < 0.01$). This is expected because the assumed velocity, Eq. (19), and temperature, Eq. (20), profiles are in error for small values of ξ . It is seen from Fig. 6 that, as Prandtl numbers decrease, the Nusselt numbers decrease and the variation of Nu with ξ becomes smaller.

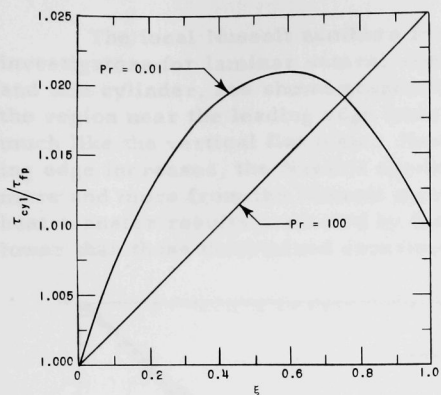


Fig. 5

Comparison of Local Shear Stress
between Cylinder and Flat Plate

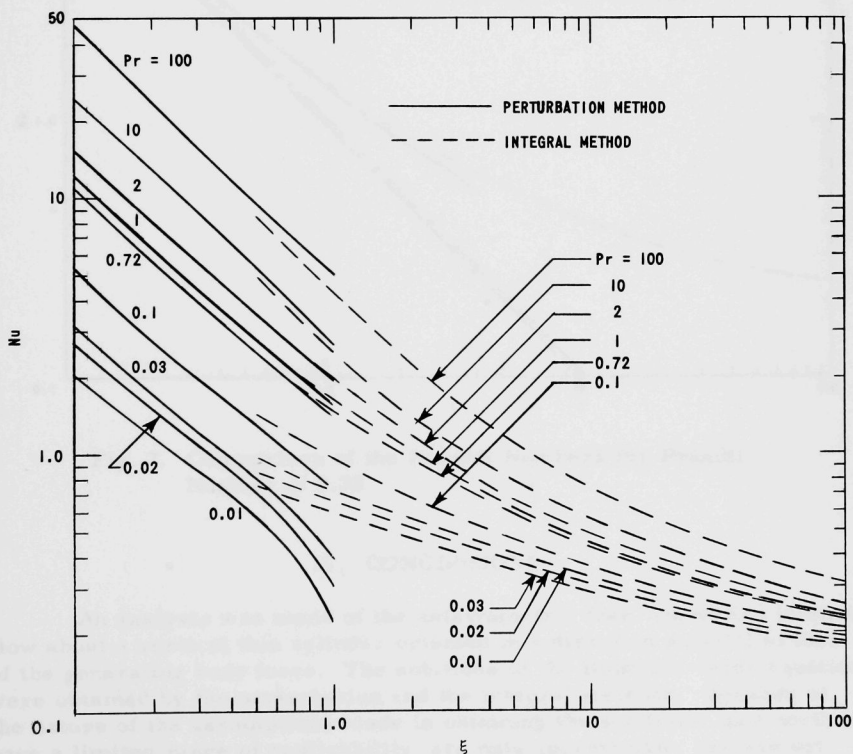


Fig. 6. Variation of the Nusselt Number for the Cylinder
Versus the x-parameter

The local Nusselt numbers for air, $Pr = 0.72$, predicted by various investigators for laminar natural-convection flow along a vertical flat plate and thin cylinder, are shown graphically in Fig. 7 as a function of ξ . In the region near the leading edge (small ξ), the vertical cylinder behaves much like the vertical flat plate. However, as the distance from the leading edge increases, the Nusselt numbers for the vertical cylinder deviate more and more from the Nusselt numbers for the flat plate. For air, the heat-transfer results predicted by the boundary-layer analysis⁽¹⁾ are lower than those determined experimentally.⁽²⁾

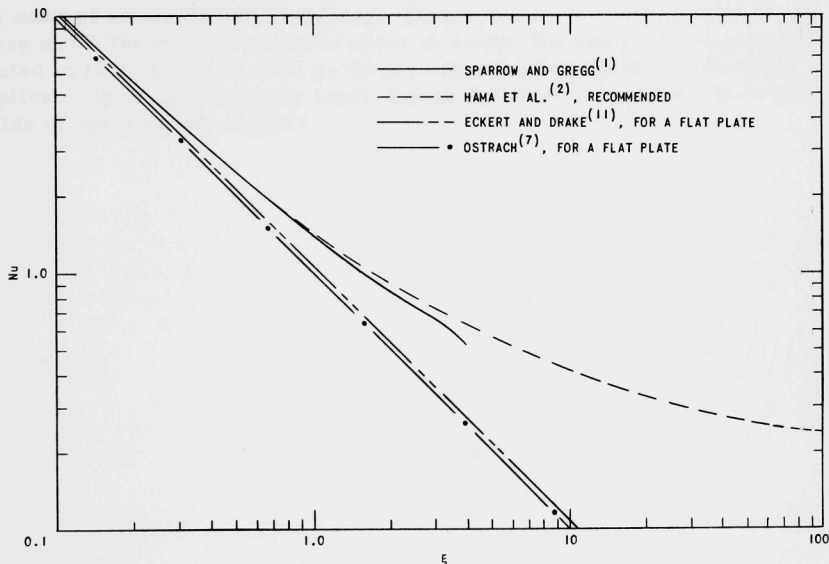


Fig. 7. Comparison of the Nusselt Numbers for Prandtl Number of 0.72.

IV. CONCLUSIONS

An analysis was made of the axisymmetric free-convection laminar flow about a vertical thin cylinder oriented in a direction parallel to that of the generating body force. The solutions of the boundary-layer equations were obtained by the perturbation and the integral methods. Because of the nature of the assumptions made in obtaining the solutions, both methods have a limited range of applicability, are only approximate, and are not expected to be very reliable for small Prandtl numbers.

The use of flat-plate Nusselt numbers for predicting heat transfer from a cylinder will always be conservative. The heat-transfer coefficients calculated will be more conservative for small Prandtl numbers than for large Prandtl numbers.

For the problem considered here, the boundary layer can become relatively thick and certain assumptions of the theory will no longer be valid. The velocity and temperature profiles assumed are not quite accurate for small values of the x -parameter ξ . In addition, the use of these profiles in the integral method of solution might not have been appropriate for the case of small Prandtl numbers. Hence, there remains a need for a more exact theory and an experiment to verify the analytical results presented in this report as well as to provide information on the limits of applicability of the boundary layer theory for free-convection flows with fluids of low Prandtl number.

APPENDIX A

NUMERICAL SOLUTION OF THE PERTURBATION EQUATIONS
[Eqs. (13) and (14)]

Inspection of both equations designated Eq. (13), for example, reveals that f_1 and θ_1 appear in both equations, which necessitates simultaneous solution. In addition, it should be noted that it is also necessary to utilize both solutions of Eq. (12) as input data, since f_0 , f_0' , f_0'' , f_0''' , θ_0' , and θ_0'' all appear in both equations of Eq. (13). In order to carry out the integrations of both equations of Eq. (13), the values f_1 , f_1' , f_1'' , θ_1 , and θ_1' are required at $\eta = 0$. From the listing of the boundary conditions, Eq. (13a), it is seen that only f_1 , f_1' , and θ_1 are given at $\eta = 0$, whereas f_1'' and θ_1' are given at $\eta \rightarrow \infty$. Thus, the computational problem is reduced to a search for the correct values of $f_1''(0)$ and $\theta_1'(0)$ which would yield a solution of the equations satisfying the boundary condition at $\eta \rightarrow \infty$ within the prescribed accuracy.

A double-precision Adams-Moulton forward-integration method was chosen for the solution of the equations. The problem was programmed for an IBM-704 digital computer. To satisfy the boundary conditions at $\eta \rightarrow \infty$, a continuous iterative process developed by Hering⁽¹⁵⁾ to obtain initial values of $f_0''(0)$ and $\theta_1'(0)$ was used. Since the tables^(7,8) of the functions f_0 , f_0' , f_0'' , θ_0 , and θ_0' were not adequate for the integrations of Eqs. (13) and (14), as the increments in the independent variable were too large, Eq. (12) was also solved. The solution thus obtained was utilized in Eqs. (13) and (14). The method of solution of Eq. (14) was identical with that of Eq. (13).

For $Pr \leq 0.1$, the functions $f_0''(\eta)$, $f_1''(\eta)$, and $f_2''(\eta)$ had a tendency to oscillate at some point ($\eta > 0$), and these oscillations grew and fed into other functions. The smaller the Prandtl number, the earlier in the integration process did the oscillations appear. This was partly due to the numerical integration method used. By decreasing the increment size this difficulty was overcome. However, for small Prandtl numbers the method of solution was extremely time consuming.

APPENDIX B REDUCTION OF THE INTEGRAL EQUATIONS [Eqs. (17) and (18)]

By substituting $y = r_0 (e^{\sigma'} - 1)$ and the velocity, Eq. (19), and temperature, Eq. (20), distributions in the integral Eqs. (17) and (18), there results

$$\begin{aligned} r_0^2 K^2 \frac{d}{dx} \int_0^\sigma [U^2 - 2U(e^{\sigma'} - 1) + (e^{\sigma'} - 1)^2] (\sigma')^2 e^{2\sigma'} d\sigma' \\ = r_0^2 g \beta |T_w - T_a| \int_0^\sigma \left(e^{2\sigma'} - \frac{\sigma'}{\sigma} e^{2\sigma'} \right) d\sigma' - \gamma KU \end{aligned} \quad (37)$$

and

$$r_0^2 K \frac{d}{dx} \int_0^\sigma \left[(U+1)\sigma' - \sigma' e^{\sigma'} - (U+1) \frac{(\sigma')^2}{\sigma} + \frac{(\sigma')^2 e^{\sigma'}}{\sigma} \right] e^{2\sigma'} d\sigma' = \frac{r_0 \alpha}{\sigma}, \quad (38)$$

respectively. Performing the indicated integrations, differentiating Eqs. (37) and (38) explicitly, and rearranging terms, one obtains

$$a \frac{dU}{dx} + b \frac{d\sigma}{dx} = c \quad (39)$$

and

$$A \frac{dU}{dx} + B \frac{d\sigma}{dx} = C, \quad (40)$$

where

$$a = \left\{ \frac{2}{3} \left[\sigma \left(\frac{2}{3} - \sigma \right) - \frac{2}{9} \right] e^{3\sigma} + (U+1) \left(\sigma^2 - \sigma + \frac{1}{2} \right) e^{2\sigma} - \frac{U}{2} - \frac{19}{54} \right\} 2\sigma, \quad (41)$$

$$b = [\sigma^2 e^{4\sigma} - 2(U+1)\sigma e^{3\sigma} + (U+1)^2 \sigma^2 e^{2\sigma}] 2\sigma, \quad (42)$$

$$c = \frac{2\nu^2}{g\beta|T_w - T_a|r_0^4} \left[(e^{2\sigma} - 1) - 2\sigma(U+1) \right], \quad (43)$$

$$A = [\sigma + 1 + (\sigma + 1)e^{2\sigma}] \sigma, \quad (44)$$

$$B = \frac{4}{3} \left[\sigma \left(\frac{2}{3} - \sigma \right) - \frac{2}{9} \right] e^{3\sigma} + 2(U+1) \left(\sigma^2 - \sigma + \frac{1}{2} \right) e^{2\sigma} - (U+1) + \frac{8}{27} \quad (45)$$

$$C = \left(\frac{4\sigma}{Pr} \right) \frac{2\nu^2}{g\beta |T_w - T_a| r_0^4} \quad (46)$$

Introducing the x -parameter (ξ) as the independent variable, Eqs. (39) and (40) can be rewritten as

$$a \frac{dU}{d\xi} + b \frac{d\sigma}{d\xi} = d \quad (47)$$

and

$$A \frac{dU}{d\xi} + B \frac{d\sigma}{d\xi} = D \quad (48)$$

where

$$d = \frac{\xi^3}{8} [e^{2\sigma} - 1 - 2\sigma(U+1)] \quad (49)$$

and

$$D = \frac{\xi^3}{2} \left(\frac{\sigma}{Pr} \right) \quad (50)$$

REFERENCES

1. E. M. Sparrow and J. L. Gregg, Laminar Free-convection Heat Transfer from the Outer Surface of a Vertical Circular Cylinder, Trans. Am. Soc. Mech. Engrs., 78, 1823 (1956).
2. F. R. Hama, J. V. Recesso, and J. Christiansen, The Axisymmetric Free-convection Temperature Field along a Vertical Thin Cylinder, J. Aero/Space Sci., 26, 335 (1959).
3. K. Millsaps and K. Pohlhausen, The Laminar Free-convective Heat Transfer from the Outer Surface of a Vertical Cylinder, J. Aeronaut. Sci., 25, 357 (1958).
4. K. T. Yang, Possible Similarity Solutions for Laminar Free-convection on Vertical Plates and Cylinders, Trans. Am. Soc. Mech. Engrs., J. Appl. Mech., 82, 230 (1960).
5. R. A. Seban and R. Bond, Skin-friction and Heat-transfer Characteristics of a Laminar Boundary Layer on a Cylinder in Axial Incompressible Flow, J. Aeronaut. Sci., 18, 671 (1951).
6. H. R. Kelly, A Note on the Laminar Boundary Layer on a Circular Cylinder in Axial Incompressible Flow, J. Aeronaut. Sci., 21, 634 (1954).
7. S. Ostrach, An Analysis of Laminar Free-convection Flow and Heat Transfer about a Flat Plate Parallel to the Direction of the Generating Body Force, NACA Report 1111 (1954).
8. E. M. Sparrow and J. L. Gregg, Details of Exact Low Prandtl Number Boundary-layer Solutions for Forced and for Free Convection, NASA Memo 2-27-59E (1959).
9. M. B. Glauert and M. D. Lighthill, The Axisymmetric Boundary Layer on a Long Thin Cylinder, Proc. Royal Soc. (London), A230, 188 (1955).
10. R. M. Mark, Laminar Boundary Layers on Slender Bodies of Revolution in Axial Flow, GALCIT Hypersonic Res. Proj. Memo 21 (1954).
11. E. R. G. Eckert and R. M. Drake, Jr., Heat and Mass Transfer, McGraw-Hill Book Co., Inc., New York (1959), pp. 312-315.
12. W. H. Braun and J. E. Heighway, An Integral Method for Natural Convection Flows at High and Low Prandtl Numbers, NASA TN D-292 (1960).

13. W. H. Braun, S. Ostrach and J. E. Heighway, Free Convection Similarity Flows about Two-dimensional and Axisymmetric Bodies with Closed Lower Ends, Int. J. Heat and Mass Transfer, 2, 121 (1961).
14. H. J. Merk, Critical Remarks on the Thickness of Dynamic and Thermal Boundary Layers, Applied Scientific Research, 8A, 100 (1959).
15. R. G. Hering, Combined Free and Forced Convection from Bodies of Revolution, Ph.D. Thesis, Purdue University (1961).

ACKNOWLEDGMENTS

The author would like to thank Drs. P. A. Lottes and C. E. Dickerman for their interest. He also wishes to acknowledge the assistance of Mr. J. Cooper who programmed the problem on the IBM-704 digital computer and Mr. L. B. Miller who checked the mathematics involved in reducing the integral equations in Appendix B.

ARGONNE NATIONAL LAB WEST



3 4444 00008412 9

7